

BB

LPCC 94-06  
3009425

# LPCC CAEN

LABORATOIRE DE PHYSIQUE CORPUSCULAIRE

ISMRA - 3, rue du Maréchal Juin - 14050 CAEN CEDEX - FRANCE

**Azimuthal correlation functions and the energy of vanishing  
flow in nucleus-nucleus collisions**

*A. Buta, J.C. Angélique, G. Auger, G. Bizard, R. Brou, C. Cabot, Y. Cassagnou,  
E. Crema, D. Cussol, Y. El Masri, Ph. Eudes, M. Gonin, K. Hagel, Z. Y. He,  
A. Kerambrun, C. Lebrun, R. Legrain, J. P. Patry, A. Péghaire, J. Péter, R. Popescu,  
R. Régimbart, E. Rosato, F. Saint-Laurent, J. C. Steckmeyer, B. Tamain, E. Vient, R. Wada*

June 1994

LPCC 94-06

*Submitted to Nuclear Physics A*

CERN LIBRARIES, GENEVA



P00023822

INSTITUT NATIONAL  
DE PHYSIQUE NUCLEAIRE ET DE PHYSIQUE DES PARTICULES

CENTRE NATIONAL DE LA RECHERCHE SCIENTIFIQUE

INSTITUT DES SCIENCES  
DE LA MATIERE ET DU RAYONNEMENT



Téléphone : 31 45 25 00  
Télécopie : 31 45 25 49



# AZIMUTHAL CORRELATION FUNCTIONS AND THE ENERGY OF VANISHING FLOW IN NUCLEUS-NUCLEUS COLLISIONS \*

---

A. Buta<sup>1-a)</sup>, J.C. Angélique<sup>1)</sup>, G. Auger<sup>2)</sup>, G. Bizard<sup>1)</sup>, R. Brou<sup>1)</sup>,  
C. Cabot<sup>2)</sup>, Y. Cassagnou<sup>3)</sup>, E. Crema<sup>2-b)</sup>, D. Cussol<sup>1)</sup>, Y. El Masri<sup>4)</sup>, Ph. Eudes<sup>5)</sup>,  
M. Gonin<sup>6)</sup>, K. Hage<sup>6)</sup>, Z.Y. He<sup>8)</sup>, A. Kerambrun<sup>1)</sup>, C. Lebrun<sup>5)</sup>, R. Legrain<sup>3)</sup>,  
J.P. Patry<sup>1)</sup>, A. Péghaire<sup>2)</sup>, J. Péter<sup>1)</sup>, R. Popescu<sup>1-a)</sup>, R. Regimbart<sup>1)</sup>, E. Rosato<sup>7)</sup>,  
F. Saint-Laurent<sup>2)</sup>, J.C. Steckmeyer<sup>1)</sup>, B. Tamain<sup>1)</sup>, E. Vient<sup>1)</sup>, R. Wada<sup>6)</sup>

- 1) LPC Caen, IN2P3-CNRS, ISMRA-Université de Caen, Boulevard Maréchal Juin, 14050 CAEN, FRANCE,
  - 2) GANIL, Boulevard Henri Becquerel, 14021 CAEN, FRANCE,
  - 3) DAPNIA, CEN Saclay, 91191 GIF S/Yvette, FRANCE,
  - 4) Institut de Physique Nucléaire, Université Catholique de Louvain, B-1348 LOUVAIN-LA-NEUVE, BELGIUM,
  - 5) Laboratoire de Physique Nucléaire, 2 rue de la Houssinière, 44072 NANTES, FRANCE,
  - 6) Cyclotron Institute, Texas A&M University, COLLEGE STATION, U.S.A.,
  - 7) Dipartimento di Scienze Fisiche, NAPOLI, ITALY,
  - 8) Institute of Modern Physics, Lanzhou University, LANZHOU, CHINA,
- a) Institutul de Fizică și Inginerie Nucleară, P.O. Box MG-6, BUCUREȘTI, ROMANIA  
b) Instituto de Física, Universidade de SAO PAULO, BRAZIL.

## Abstract :

A novel method is proposed for studying the evolution of flow phenomena with the incident energy, and for quantitatively estimating the energy of vanishing flow (also called balance energy,  $E_{bal}$ ) without reconstructing the reaction plane. We used a method based on the shapes of experimental particle-particle azimuthal correlation functions to determine  $E_{bal}$  for three systems : Ar+Al, Zn+Ti, Zn+Ni. We compare the results with estimations using flow parameter analysis and also with theoretical expectations.

## 1. INTRODUCTION

Heavy ion reactions at incident energies ranging from about 10 MeV/u up to a few hundreds of MeV/u are important in the study of nuclear matter because the nuclear interaction changes from attractive to repulsive in this region. At incident energies up to a few tens of MeV/u the interaction is dominated by the attractive mean field giving rise to a partial orbiting and a deflection of the participating nucleons and clusters to negative angles. Conversely, at a few hundreds of MeV/u the interaction is dominated by the repulsive core of the nucleon-nucleon interaction and compression occurs. The interaction can then be visualized as two nuclei bouncing off each other and the participating nucleons in the interaction region are deflected to positive angles [1].

\* Experiment performed at GANIL.

The directed collective motion of these nucleons and clusters in the reaction plane (sideways flow) is then a signature of the interaction and can provide informations about the nuclear equation of state (EOS). In recent years much effort has been done for measuring this collective flow and several groups have performed experiments to study the transition from negative flow (at low energies) to positive flow (at high energies) [2-6].

The disappearance of collective flow, corresponding to the point where the attractive scattering balances the repulsive interactions, is predicted to appear at some incident energy-termed balance energy  $E_{bal}$  [3], or energy of vanishing flow EVF [7] - . The determination of  $E_{bal}$  is important because the magnitude of parameters in the EOS can be related to the relative contributions of repulsive or attractive scattering. Both in [5] and [6] a systematic study of flow phenomena has been performed for various nuclear systems and  $E_{bal}$  has been estimated from the variation of the flow parameter with incident energy. A linear dependence of  $E_{bal}$  on  $A^{-1/3}$ , initially predicted in [7] has been noted.

Another type of analysis which can yield information about the changes in reaction dynamics over this transitional region is the study of azimuthal distributions which contain other signatures of the collective flow [8-11]. At high incident energies, the azimuthal distributions exhibit maxima at angles perpendicular to the reaction plane. This anisotropy is due to collective effects such as squeeze-out [12-13]. On the contrary, at incident energies of a few tens of MeV/u, the azimuthal distributions have maxima in the reaction plane ("rotation-like" behaviour [14-15] in addition to the sideways flow).

Both types of analyses, the flow parameter determination and the azimuthal distribution measurements, require the knowledge of the reaction plane and their results should be corrected for the uncertainties related to the reconstruction of the reaction plane from the detected reaction products [1]. Even with a good quality  $4\pi$  detector these uncertainties could be quite large [16].

One way to avoid this difficulty is to study particle-particle azimuthal correlation functions. This type of analysis does not require the knowledge of the reaction plane and the shape of azimuthal correlation functions was shown to be sensitive to the EOS [17]. An additional benefit of the correlation function method, also noted in [17], is that it allows one to confine the analysis to an acceptance region where the detector efficiency is high. Recently [18] the shape of particle-particle correlation functions for Ar+Sc in the energy range 35-115 MeV/u have been qualitatively analyzed in terms of two components : collective flow and rotational collective motion.

Here we show that the shapes of azimuthal correlation functions are sensitive both to the direction of the collective flow and to its intensity. Then by studying the evolution with the incident energy of these shapes we develop a method for estimating the energy of vanishing flow and apply it for three nuclear systems studied at GANIL.

## 2 - EXPERIMENTS AND SELECTION CRITERIA

The experimental data analyzed in this report have been measured at GANIL. The nuclear reactions were  $^{36}\text{Ar} + ^{27}\text{Al}$  between 55 MeV/u and 95 MeV/u,  $^{64}\text{Zn} + ^{48}\text{Ti}$  and  $^{64}\text{Zn} + ^{58}\text{Ni}$  between 35 MeV/u and 79 MeV/u.

The charges and velocities of nearly all charged products were measured on an event by event basis with a  $4\pi$  plastic scintillator array. This axially symmetric multidetector consists in the MUR [19] which covers polar angles from  $3.2^\circ$  to  $30^\circ$  and the TONNEAU [20] which covers polar angles from  $30^\circ$  to  $150^\circ$ . Due to electron contamination, the  $Z = 1$  spectra in the two innermost rings of the MUR were perturbed. In addition, these two rings have an azimuthal resolution of  $\pm 22^\circ$ , and we preferred to disregard them, reducing the polar angle acceptance of the MUR to a  $7.3^\circ$  to  $30^\circ$  interval. The first step in the analysis was to select well characterized events by requiring that the total parallel momentum of all detected products amounts for more than 60 % of the projectile linear momentum [21].

Then, the events have been sorted with respect to the impact parameter. Two global variables have been used to estimate the impact parameter : the total transverse momentum and the average parallel velocity [21] which give nearly identical results. The final analysis was done for events in three intervals of experimentally estimated impact parameter : central ( $b_{\text{exp}} < 2.5$  fm), mid-central ( $2.5 < b_{\text{exp}} < 4.5$  fm) and mid-peripheral ( $4.5 < b_{\text{exp}} < 6.5$  fm).

The particles in each event have been classified in three rapidity intervals. Denoting by  $Y_r = Y / Y_{\text{beam}}$  the rapidity of a particle relative to the beam rapidity, the three intervals were : 0.0 - 0.35, 0.35 - 0.65 and 0.65 - 1.0. Two particles are said to belong to the same class if they belong simultaneously to the same interval of impact parameter and to the same interval of rapidity. Most of the particles have charge one or two, less than 5 % of them having larger charges.

For particles in the same class as defined above, we define the experimental azimuthal correlation function in the usual way [17] :

$$C(\Delta\Phi) = P_{\text{corr}}(\Delta\Phi) / P_{\text{uncorr}}(\Delta\Phi) \quad (1)$$

Here  $\Delta\Phi$  is the difference of azimuthal angles  $\Phi_1$  and  $\Phi_2$  of two particles (i.e. the angle between their transverse momenta),  $P_{\text{corr}}$  is the observed distribution for pairs in which both particles belong to the same event,  $P_{\text{uncorr}}$  is the distribution for uncorrelated pairs generated by event mixing, i.e., each particle from a pair is randomly chosen from different events belonging to the same class, excluding the pairs leading to two particles in the same detector.

Fig. 1 displays an example of  $P_{\text{corr}}(\Delta\Phi)$ ,  $P_{\text{uncorr}}(\Delta\Phi)$  and  $C(\Delta\Phi)$  for the 55 MeV/u Ar + Al system in the 4.5 - 6.5 fm impact parameter bin and the 0 - 0.35 rapidity

interval.  $P_{\text{uncorr}}$  is an almost isotropic distribution except at small values of  $\Delta\Phi$ , where the decreasing is due to the effect of the finite azimuthal resolution of the detectors. This decreasing is no longer visible in the  $C(\Delta\Phi)$  distribution, proving that the uncorrelated azimuthal distribution was correctly determined and allowed to eliminate most of the experimental limitations.

### 3- THE METHOD USED FOR $E_{\text{bal}}$ DETERMINATION.

Typical azimuthal correlation functions are shown in fig. 2 and 3 for Ar + Al at 55 MeV/u for the three intervals of impact parameter and for the three intervals of rapidity defined previously. All types of particles have been considered together to construct  $C(\Delta\Phi)$  except in the right column of fig. 2 where we have selected pairs with at least one charge 2 particle. For the experimental correlation functions which have been constructed according to (1), we made a fit with the expression :

$$C(\Delta\Phi) = A (1 + \lambda_1 \cos\Delta\Phi + \lambda_2 \cos 2\Delta\Phi) \quad (2)$$

As we will see later,  $\lambda_2$  in this data is always much less than 1.  $\lambda_1$  is therefore directly related to the  $0^\circ - 180^\circ$  asymmetry of  $C(\Delta\Phi)$  :

$$\lambda_1 = (C(0^\circ) - C(180^\circ)) / (C(0^\circ) + C(180^\circ)) \quad (3)$$

If  $\lambda_1 > 0$ ,  $C(\Delta\Phi)$  has a maximum at  $0^\circ$ ; on the contrary, if  $\lambda_1 < 0$ , the correlation function has a maximum at  $180^\circ$ .

Recalling the ratio  $R = C(0^\circ) / C(180^\circ)$ , we note that :

$$R - 1 = 2\lambda_1 / (1 - \lambda_1) \simeq 2\lambda_1 \quad (4)$$

The  $\lambda_2$  parameter is related in a similar way to the  $0^\circ - 90^\circ$  asymmetry ;

$$\lambda_2 = \frac{C(0^\circ) + C(180^\circ) - 2 C(90^\circ)}{C(0^\circ) + C(180^\circ) + 2 C(90^\circ)} \quad (5)$$

in all of our data,  $\lambda_2$  is always  $> 0$  so we have always  $C(180^\circ) + C(0^\circ) > 2 C(90^\circ)$ .

We show in this analysis that the evolution of  $\lambda_1$  with energy can be used to extract  $E_{\text{bal}}$ .

If particles in an event are emitted independently with the same azimuthal distribution  $F(\Phi)$ , it can be shown mathematically that the correlation function  $C(\Delta\Phi)$  is related to  $F(\Phi)$  by :

$$C(\Delta\Phi) = \int_0^{360^\circ} F(\Phi) F(\Phi+\Delta\Phi) d\Phi \quad (6)$$

$C(\Delta\Phi)$  should always have a maximum at  $\Delta\Phi = 0^\circ$ , except for the trivial case when  $F(\Phi)$  is a constant which leads then to constant  $C(\Delta\Phi)$ . Other maxima will appear in  $C(\Delta\Phi)$  for periodic  $F(\Phi)$ , but their magnitude will never exceed  $C(0^\circ)$  ( for instance, if  $F(\Phi + 180^\circ) = F(\Phi)$ ,  $C(180^\circ) = C(0^\circ)$  )

To illustrate the physical meaning of  $C(\Delta\Phi)$  and its links with the sideward flow, we will consider a simplified geometrical picture of the dynamical evolution of the interaction in our energy region, as shown in fig. 4, in the centre of mass frame. The projectile P moves from left to right along the Z axis, XOY being the plane perpendicular to the beam direction. In the center of each figure are shown the linear momenta for particles, projected onto the reaction plane, XOZ. The same linear momenta projected onto a plane perpendicular to the beam axis (XOY) are the transverse momenta. They are shown on the left and right parts of this figure for particles with rapidity  $Y < Y_{cm}$  (left) and for particles with  $Y > Y_{cm}$  (right). We will focus our attention on the particles moving backwards in the centre of mass (rapidity  $Y < Y_{cm}$ ), but the conclusions are identical for the  $Y > Y_{cm}$  region.

For incident energies  $E \ll E_{bal}$ , where the interaction is dominated by the mean field, attractive scattering deflects the particles with  $Y < Y_{cm}$  mostly in the projectile direction in the reaction plane. That means their transverse momenta are confined to a more or less narrow cone with its axis in the reaction plane : fig 4a.

The same behaviour is expected at incident energies  $E \gg E_{bal}$  where dominant repulsive scattering (fig. 4c) deflects particles with  $Y < Y_{cm}$  in the reaction plane in the direction opposite to the projectile direction and their transverse momenta are confined to a narrow cone.

Contrary to these two situations, at  $E = E_{bal}$ , the two effects balance each other, the flow is 0. so that particles with  $Y < Y_{cm}$  will be deflected symmetrically in the reaction plane as displayed in fig. 4b.

The effect of these changes on the azimuthal correlation functions can be estimated by making a simple calculation : suppose we have n particles in an event with their transverse momenta randomly distributed in two opposite cones of aperture angle  $\delta f$ , but always  $n_1$  particles in the first cone and  $n_2$  in the other. Physically,  $\delta f$  represents the focussing around the reaction plane : small  $\delta f$  values mean strong focussing,  $\delta f = 90^\circ$  means uniform azimuthal distribution. Of course,  $n_1 + n_2 = n$ .

The number of different particle pairs correlated at small angles is :

$$N(0^\circ) = n_1 (n_1 - 1) / 2 + n_2(n_2 - 1) / 2 \quad (7)$$

whereas the number of different particle pairs correlated at large angles is :

$$N(180^\circ) = n_1 n_2 \quad (8)$$

Fig.5 shows the results of a simulation where we generated events with multiplicity  $n = 6$ . The azimuthal angles of successive particles are randomly chosen following a distribution law  $F(\Phi)$  defined as follows :  $F(\Phi)$  is uniform in the  $-\delta f, +\delta f$  interval, and also in the  $180^\circ - \delta f, 180^\circ + \delta f$  interval and the ratio  $F(0^\circ) / F(180^\circ)$  is fixed by the in-plane asymmetry of the particles :  $F(0^\circ) / F(180^\circ) = \langle n_1 \rangle / \langle n_2 \rangle$ . The three columns in fig.5 correspond to  $\langle n_1 \rangle = 1, 2, 3$  and the three rows correspond to different cone angles.  $\lambda_1$  is never negative and reaches its minimum value 0. for the symmetric distribution  $\langle n_1 \rangle = \langle n_2 \rangle = n / 2$ .

In fig. 5, in agreement with formula 6, the maximum of the  $\Delta\Phi$  distribution is always at  $\Delta\Phi = 0^\circ$ . However, physical reasons, such as conservation laws, may constrain the emission angles of the different particles in an event and violate the independence hypothesis leading to formula 6. Then,  $C(\Delta\Phi)$  may reach its maximum at  $\Delta\Phi = 180^\circ$ . This is illustrated in fig. 6 which is identical to fig. 5 except that only one configuration has been retained for each column, for example  $n_1 = n_2 = 3$  in the third column, instead of  $\langle n_1 \rangle = \langle n_2 \rangle = 3$  for fig. 5. Now  $\lambda_1$  can take negative values but the same conclusion hold for the simulation of fig. 6 as for that of fig. 5 : for a given value of  $\delta f$ ,  $\lambda_1$  reaches a minimum for the symmetric distribution  $n_1 = n_2 = n/2$ .

To summarize,  $\lambda_1$  decreases with increasing  $E$  for  $E < E_{bal}$ , reaches a minimum when  $E = E_{bal}$  where symmetric scattering occurs and then increases with increasing  $E$  for  $E > E_{bal}$ .

We therefore follow the evolution of  $\lambda_1$  with incident energy and determine  $E_{bal}$  to be the energy at which  $\lambda_1$  has a minimum value.

#### 4- EXPERIMENTAL RESULTS CONCERNING $E_{bal}$

The changes of shape of the correlation function  $C(\Delta\Phi)$  and hence of the asymmetry coefficient  $\lambda_1$  (or  $R$ ) as a function of the incident energy are illustrated in figure 7, for the Ar + Al system. All values of  $\lambda_1$ , for the different systems, and the different impact parameter intervals are shown in figure 8, for relative rapidities in the 0. - .35. interval.

One clearly observes for central collisions the evolution of  $\lambda_1$  which one expects from the considerations made in the previous chapter : that is a decrease with the incident energy, a minimum and then an increase. If we examine the experimental points, we note a systematic increase of the position of the minimum with the impact parameter for each



system. The minimum is just reached or beyond the available range of incident energies for mid-central and mid-peripheral collisions.

The variations of  $\lambda_1$  with energy were fitted with a 2-degree polynomial to determine  $E_{bal}$  from the position of the minimum. As indicated previously, these values of  $E_{bal}$  concern particles having  $Z = 1, 2$  or  $3$ . Is  $E_{bal}$  sensitive to the nature of the particles used to construct  $C(\Delta\Phi)$ ? We have seen in fig. 2 that  $\lambda_1$  changes substantially when pairs with at least one  $Z = 2$  particle are selected. However, with or without any condition on the particles, the relative variations of  $\lambda_1$  with energy are somewhat similar, as can be seen in figure 9 : there is no evidence for an  $E_{bal}$  dependence on the nature of the particles.

We compare in figure 10 our estimations of  $E_{bal}$  to those obtained from standard flow parameter analyses [3, 4, 5, 22, 23]. One can see a good agreement of our present estimations with the previous results as well as with theoretical LVUU calculations using the standard Gogny force with an incompressibility modulus  $K_\infty = 223$  MeV (open points [7]). The dashed curve is obtained from the theoretical points assuming empirically a linear  $A^{-1/3}$  dependence.

Before leaving this section, let us make two important remarks :

- as already shown in figure 3, it is clear from figure 7 that the experimental data do show examples of negative  $\lambda_1$ . This same feature in contradiction with formula 6, has already been noted by others authors [18, 24, 25] who invoke final state interactions between particles and/or momentum conservation laws, the effects of which superimpose  $C(\Delta\Phi)$  derived in formula 6. Provided this superimposition, whatever its origin, does not vary rapidly in this energy region, the value of  $E_{bal}$  extracted using our procedure will not be affected.

- $E_{bal}$  can, in principle, also be determined by performing the same analysis using large rapidity particles. There are, however, problems associated with the non-symmetric experimental set-up with respect to the detection of particles near the projectile and target rapidities. The velocity threshold of the MUR and TONNEAU differ, and the  $\phi$  resolution varies from  $\pm 5^\circ$  at backward angles to  $\pm 22.5^\circ$  at the most forward angles. In addition, the backward hole in the TONNEAU and the forward hole in the MUR affect differently the two rapidity domains. All of this lead to a poorer resolution of  $\lambda_1$  in the rapidity interval of  $.65 - 1$ , as compared with lower rapidity interval of  $0. - .35$ . We illustrate in figure 11 that the values of  $E_{bal}$  using the largest rapidity particles are nevertheless comparable with the values of  $E_{bal}$  extracted from figure 8.

## 5- CONCLUSIONS

We have reported on a novel method for studying the evolution of the flow phenomena with the incident energy, and for quantitatively estimating the energy of

vanishing flow,  $E_{bal}$ . The method uses the  $0^\circ - 180^\circ$  asymmetry of the particle - particle azimuthal correlation function, and does not need the knowledge of the reaction plane.

The asymmetry  $0^\circ - 180^\circ$  of this correlation function is shown to be related to the absolute magnitude of the sideways flow.

There is a good agreement between the values of  $E_{bal}$  determined with our method and those extracted from standard transverse momentum analysis. The values of  $E_{bal}$  determined in this way for three nuclear systems confirm an increase with the impact parameter and show apparently no dependence on the mass of the correlated particles. The evolution of  $E_{bal}$  with the total mass of the nuclear system shows the  $A^{-1/3}$  dependence noted previously both in calculations and experimental data.

The azimuthal correlation analysis proves to be effective for qualitatively understanding flow phenomena and also for quantitatively estimating physical quantities of interest.

## FIGURE CAPTIONS

Figure 1 : From top to bottom :

- the measured  $\Delta\Phi$  distribution for correlated pairs  $P_{\text{corr}}(\Delta\Phi)$
- the measured  $\Delta\Phi$  distribution for uncorrelated pairs  $P_{\text{uncorr}}(\Delta\Phi)$
- the correlation function  $C(\Delta\Phi)$

for the 55 MeV/u Ar + Al system, mid-peripheral events, first rapidity interval  
( $0. < Y_{\text{T}} < .35$  )

Figure 2 : The correlation functions  $C(\Delta\Phi)$ , for the 55 MeV/u Ar + Al system, three intervals of impact parameter, first interval of rapidity. Left column : no condition on the particle pairs. Right column : at least one particle of the pair has an electric charge equal to two. The fits are obtained following formula (2). The values of  $\lambda_1$  are indicated on the figure.

Figure 3 :  $C(\Delta\Phi)$  for the 55 MeV/u Ar + Al system, in three intervals of impact parameter, and for the last two intervals of rapidity, without conditions on the pairs of particles.

Figure 4 : Schematic representation of the sideways flow in the CM system for three incident energies :  $E \ll E_{\text{bal}}$  (a),  $E = E_{\text{bal}}$  (b) and  $E \gg E_{\text{bal}}$  (c). The central part is the projection of the linear momenta on the reaction plane. The left and right parts are transverse momenta for  $Y < Y_{\text{cm}}$  and for  $Y > Y_{\text{cm}}$  respectively.

Figure 5 : The correlation functions  $C(\Delta\Phi)$  obtained in a simulation distributing six particles in two opposite cones of aperture  $\delta f$  (see text).

Figure 6 : Same as figure 5, but for fixed distributions (for example,  $n_1 = 1$  means that one particle is emitted in one cone, and the five remaining particles in the second cone as illustrated by the diagrams in the upper part of the figure - for these diagrams, we have chosen  $\delta f = \pm 45^\circ$ ).

Figure 7 : The correlation functions for particles from the Ar + Al system at three incident energies, for the first interval of rapidity ( $0 < Y_{\text{T}} < 0.35$ ) and central events ( $b_{\text{exp}} < 2.5$  fm).

Figure 8 : Evolution of  $\lambda_1$  as a function of energy for the three systems Ar + Al , Zn + Ti , Zn + Ni, the three intervals of impact parameters and the first rapidity interval.

The curves correspond to parabolic fits of the data. The best value of the position of the minimum of  $\lambda_1$  is indicated on the figure.

Figure 9 : The evolution of  $\lambda_1$  with incident energy for low rapidity particles ( $Y_{\text{T}} = 0 - 0.35$ ). Panel a : Zn + Ni system. Panel b : Ar + Al system. In both panels, full circles

correspond to  $\lambda_1$  when  $Z = 1, 2, 3$  are used to construct  $C(\Delta\Phi)$ , the full triangles correspond to  $\lambda_1$  obtained when at least one of the particle in each pair has a charge  $Z = 2$ .

Figure 10 : Comparisons of our estimations of  $E_{ba1}$  with results obtained from transverse momentum analysis and theoretical calculations (see text) : triangles : experimental results from [3, 22, 23] ; closed circles : experimental results from [4, 5] ; closed bars : present work ; open circles : LVUU calculations. The dashed line is a linear fit, close to  $A^{-1/3}$ , to the open circles.

Figure 11 : The evolution of  $\lambda_1$  with the incident energy for Ar + Al system and two intervals of rapidity :  $Y_T = 0 - 0.35$  (left part) and  $Y_T = 0.65 - 1$  (right part). The estimated impact parameter  $b_{exp}$  is indicated in each panel.

## REFERENCES

1. P. Danielewicz and Odyniec,  
Phys. Lett. B157 (1985) 146
2. J.P. Sullivan, J. Péter, D. Cussol, G. Bizard, R. Brou, M. Louvel, J.P. Patry, R. Regimbart, J.C. Steckmeyer, B. Tamain, E. Créma, H. Doubre, K. Hagel, G.M. Jin, A. Péghaire, F. Saint-Laurent, Y. Cassagnou, R. Legrain, C. Lebrun, E. Rosato, R. Mc Grath, S.C. Jeong, S.M. Lee, Y. Nagashima, T. Nakagawa, M. Ogihara, J. Kasagi and T. Motobayashi,  
Phys. Lett. B249 (1990) 8
3. C.A. Ogilvie, W. Bauer, D.A. Cebra, J. Clayton, S. Howden, J. Karn, A. Nadasen, A. Vander Molen, G.D. Westfall, W.F. Wilson and J.S. Winfield,  
Phys. Rev. C42, R10 (1990)
4. J. Péter  
Nucl. Phys. A545 (1992) 173c
5. J.C. Angélique, A. Péghaire, G. Bizard, C. Auger, R. Brou, A. Buta, C. Cabot, Y. Cassagnou, E. Créma, D. Cussol, Y. El Masri, Ph. Eudes, M. Gonin, K. Hagel, Z.Y. He, A. Kerambrun, C. Lebrun, R. Legrain, J.P. Patry, J. Péter, R. Popescu, R. Regimbart, F. Rosato, F. Saint-Laurent, J.C. Steckmeyer, B. Tamain, E. Vient and R. Wada,  
The XXXI International Winter Meeting on Nuclear Physics, Bormio (Italy), January 25-30 (1993)
6. G.D. Westfall, W. Bauer, D. Craig, M. Cronqvist, E. Gaultieri, S. Hannuschke, D. Klakow, T. Li, T. Reposeur, A.M. Vander Molen, W.K. Wilson, J.S. Winfield, J. Yee, S.J. Yennello, R. Lacey, A. Elmaani, J. Lauret, A. Nadaser and E. Norbeck  
Phys. Rev. Lett. 71 (1993) 1986
7. V. de la Mota, F. Sebille, M. Farine, B. Remaud and P. Schuck,  
Phys. Rev. C46 (1992) 677
8. M.B. Tsang, W. G. Lynch, C.B. Chitwood, D.J. Fields, D.R. Klesch, C.K. Gelbke, G.R. Young, T.C. Awes, R.L. Ferguson, F.E. Obenshain, F. Plasil and R.L. Robinson,  
Phys. Lett. B148 (1984) 265

9. C.B. Chitwood, D.J. Fields, C.K. Gelbke, D.R. Klesch, W.G. Lynch, M.B. Tsang, T.C. Awes, R.L. Ferguson, F.E. Obenshain, F. Plasil, R.L. Robinson and G.R. Young,  
Phys. Rev. C34 (1986) 858
10. K.G. Doss, H.A. Gustafsson, H. Gutbrod, J.W. Harris, B.V. Jacak, K.H. Kampert, B. Kolb, A.M. Poskanzer, H.G. Ritter, H.R. Schmidt, L. Teitelbaum, M. Tincknell, S. Weiss and H. Wieman,  
Phys. Rev. Lett. 59 (1987) 2720
11. G.M. Welke, M. Prakash, T.T.S. Kuo, S. Das Gupta and C. Gale,  
Phys. Rev. C38 (1988) 2101
12. M. Demoulin, D. L'Hôte, J.P. Alard, J. Augerat, R. Babinet, N. Bastid, F. Brochard, C. Cavata, N. de Marco, P. Dupieux, H. Fanet, Z. Fodor, L. Fraysse, P. Gorodetzky, J. Gosset, T. Hayashino, M.C. Lemaire, A. Le Merdy, B. Lucas, J. Marroncle, G. Montarou, M.J. Parizet, J. Poitou, C. Racca, W. Schimmerling, Y. Terrien and O. Valette,  
Phys. Rev. Lett. B241 (1990) 476
13. H.H. Gutbrod, K.H. Kampert, B.W. Kolb, A.M. Poskanzer, H.G. Ritter and H.R. Schmidt,  
Phys. Lett. B216 (1989) 267
14. W.K. Wilson, W. Benenson, D.A. Cebra, J. Clayton, S. Howden, J. Karn, T. Li, C.A. Ogilvie, A. Vander Molen, G.D. Westfall, J.S. Winfield, B. Young and A. Nadasen,  
Phys. Rev. C41 (1990) R1881
15. W.Q. Shen, J. Péter, G. Bizard, R. Brou, D. Cussol, M. Louvel, J.P. Patry, R. Regimbart, J.C. Steckmeyer, J.P. Sullivan, B. Tamain, E. Créma, H. Doubre, K. Hagel, G.M. Jin, A. Péghaire, F. Saint-Laurent, Y. Cassagnou, R. Legrain, C. Lebrun, E. Rosato, R. Mac Grath, S.C. Jeong, S.M. Lee, Y. Nagashima, T. Nakagawa, M. Ogihara, J. Kasagi and T. Motobayashi,  
Nucl. Phys. A551 (1993) 333
16. J.P. Sullivan and J. Péter,  
Nucl. Phys. A540 (1992) 275

17. S. Wang, Y.Z. Jiang, Y.M. Liu, D. Keane, D. Beavis, S.Y. Chu, S.Y. Fung, M. Vient, C. Hartnack and H. Stöcker,  
Phys. Rev. C44 (1991) 1091
18. R.A. Lacey, A. Elmaani, J. Lauret, T. Li, W. Bauer, D. Craig, M. Cronqvist, E. Gualtieri, S. Hannuschke, T. Reposeur, A. Vander Molen, G.D. Westfall, W.K. Wilson, T.S. Wienfield, J. Yee, S. Yennello, A. Nadasen, R.S. Tickle and E. Norbeck,  
Phys. Rev. Lett. 70 (1993) 1224
19. G. Bizard, A. Drouet, F. Lefebvres, J.P. Patry, B. Tamain, F. Guilbault and C. Lebrun,  
Nucl. Instr. & Meth. A244 (1986) 483
20. A. Péghaire, B. Zwieglinski, E. Rosato, G.M. Jin, J. Kasagi, H. Doubre, J. Péter, Y. Cassagnou, F. Guilbault, C. Lebrun and R. Legrain,  
Nucl. Instr. & Meth. A299 (1990) 365
21. J. Péter, D. Cussol, G. Bizard, R. Brou, M. Louvel, J.P. Patry, R. Regimbart, J.C. Steckmeyer, J.P. Sullivan, B. Tamain, E. Crema, H. Doubre, K. Hagel, G.M. Jin; A. Péghaire, F. Saint-Laurent, Y. Cassagnou, R. Legrain, C. Lebrun, E. Rosato, R. Mc Grath, S.C. Jeong, S.M. Lee, Y. Nagashima, T. Nakagawa, M. Ogihara, J. Kasagi and T. Motobayashi,  
Nucl. Phys. A519 (1990) 611
22. D. Krofcheck, W. Bauer, G.M. Grawley, C. Djalali, S. Howden, C.A. Ogilvie, A. Vander Molen, G.D. Westfall, W.K. Wilson, R.S. Tickle and C. Gale,  
Phys. Rev. Lett. 63 (1989) 2028
23. W.M. Zhang, R. Madey, M. Elaasar, J. Schambach, D. Keane, B.D. Anderson, A.R. Baldwin, J. Cogar, J.W. Watson, G.D. Westfall, G. Krebs and H. Wieman,  
Phys. Rev. C42 (1990) R491
24. T. Ethvignot, N.N. Ajitanand, J.M. Alexander, E. Bauge, A. Elmaani, L. Kowalski, M. Lopez, M.T. Magda, P. Désesquelles, H. Elhage, A. Giorni, D. Heuer, S. Kox, A. Lleres, F. Merchez, C. Morand, D. Rebreyend, P. Stassi, J.B. Viano, F. Benrachi, B. Chambon, B. Cheynis, D. Drain and C. Pastor,  
Phys. Rev. C46 (1992) 637

25. L. Phair, D.R. Bowman, N. Carlin, C.K. Gelbke, W.G. Gong, Y.D. Kim, M.A. Lisa, W.G. Lynch, G.F. Peaslee, R.T. de Souza, M. B. Tsang, C. Williams, F. Zhu, N. Colonna, K. Hanold, M.A. Mac Mahan, G.J. Wozniak, Nucl. Phys. A564 (1993) 453.



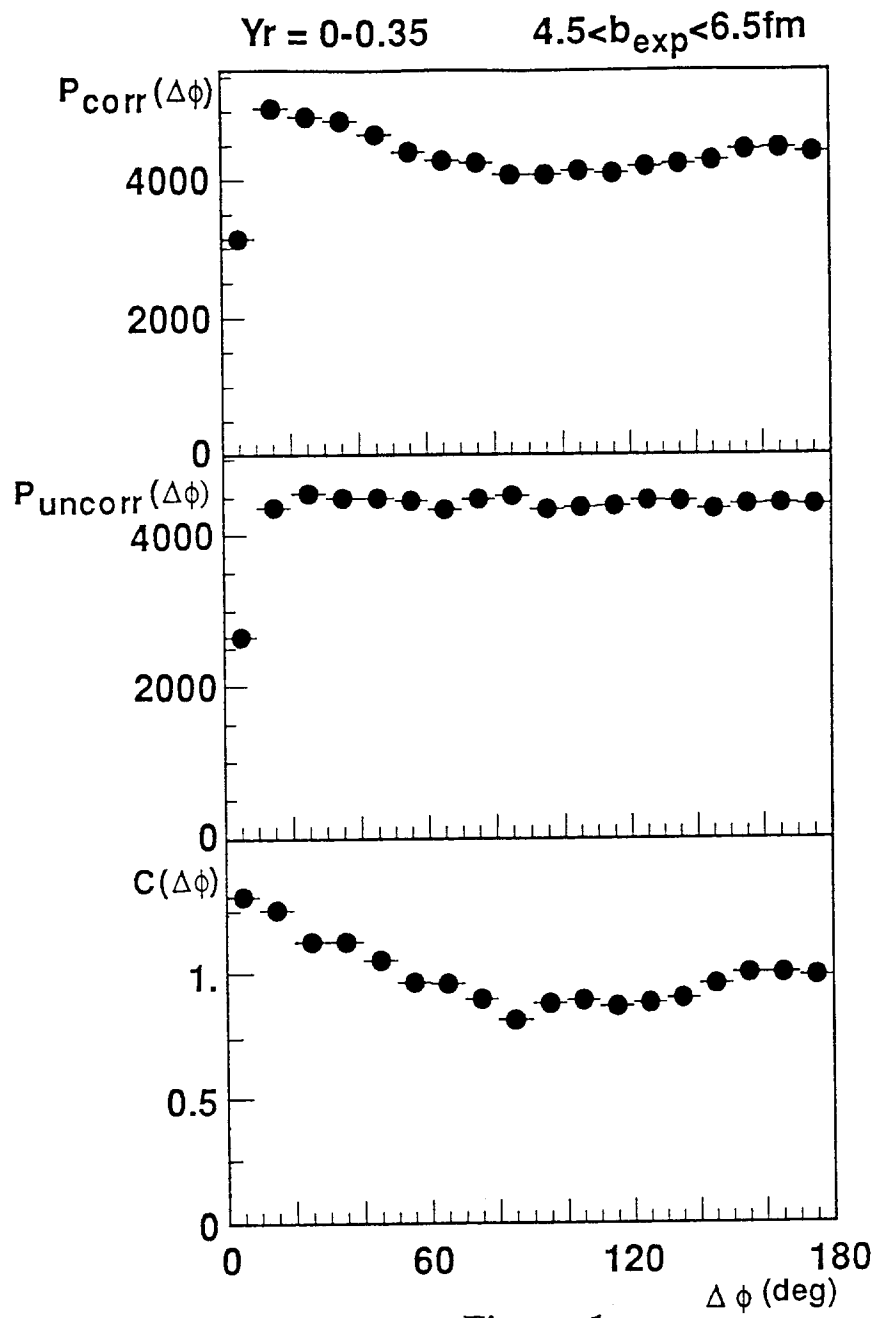


Figure 1

Ar+Al, E= 55 MeV/u / Yr=0.00-0.35

Z = 1, 2, 3

Z = 2

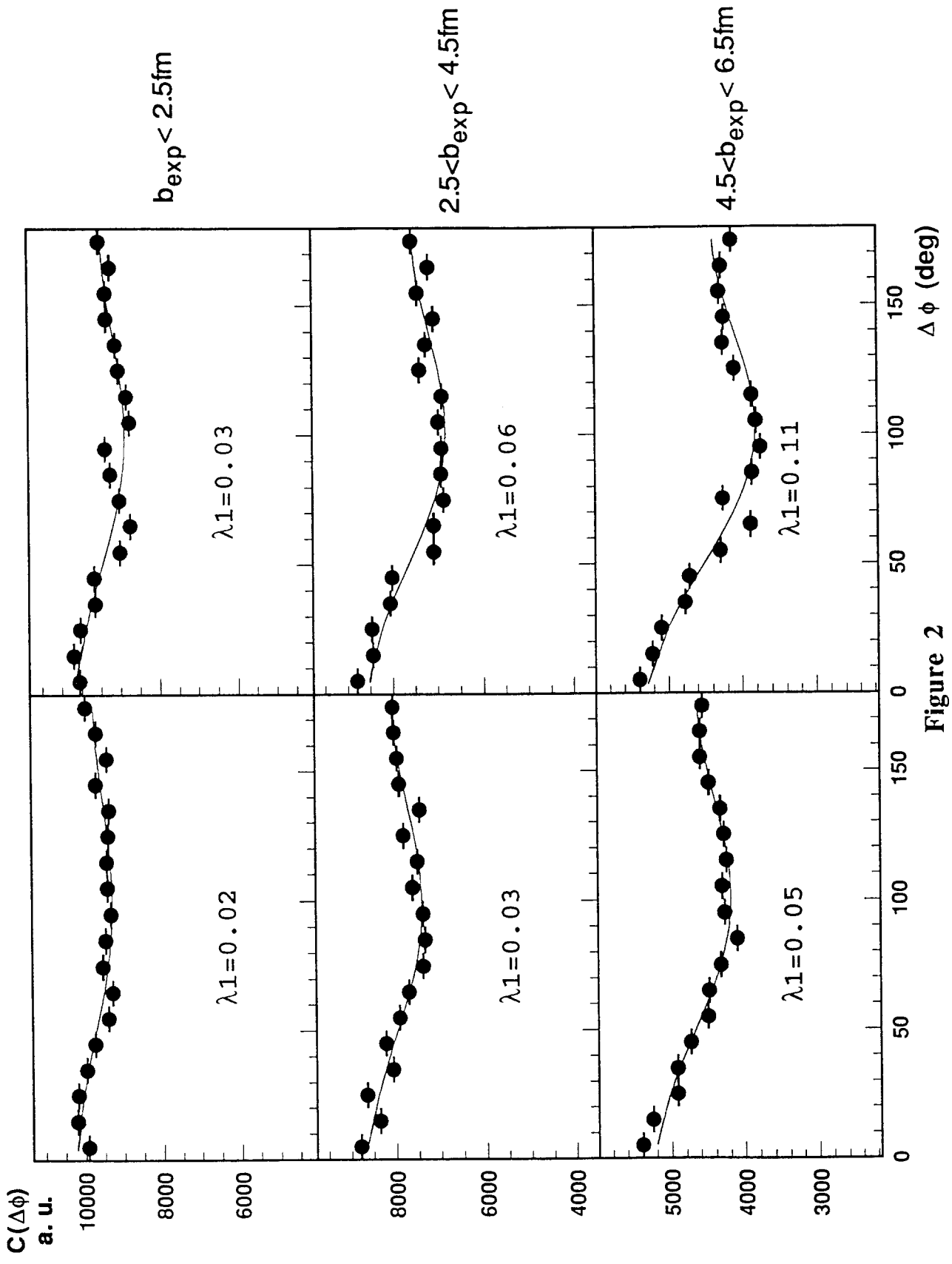


Figure 2

Ar+Al, E= 55 MeV/u

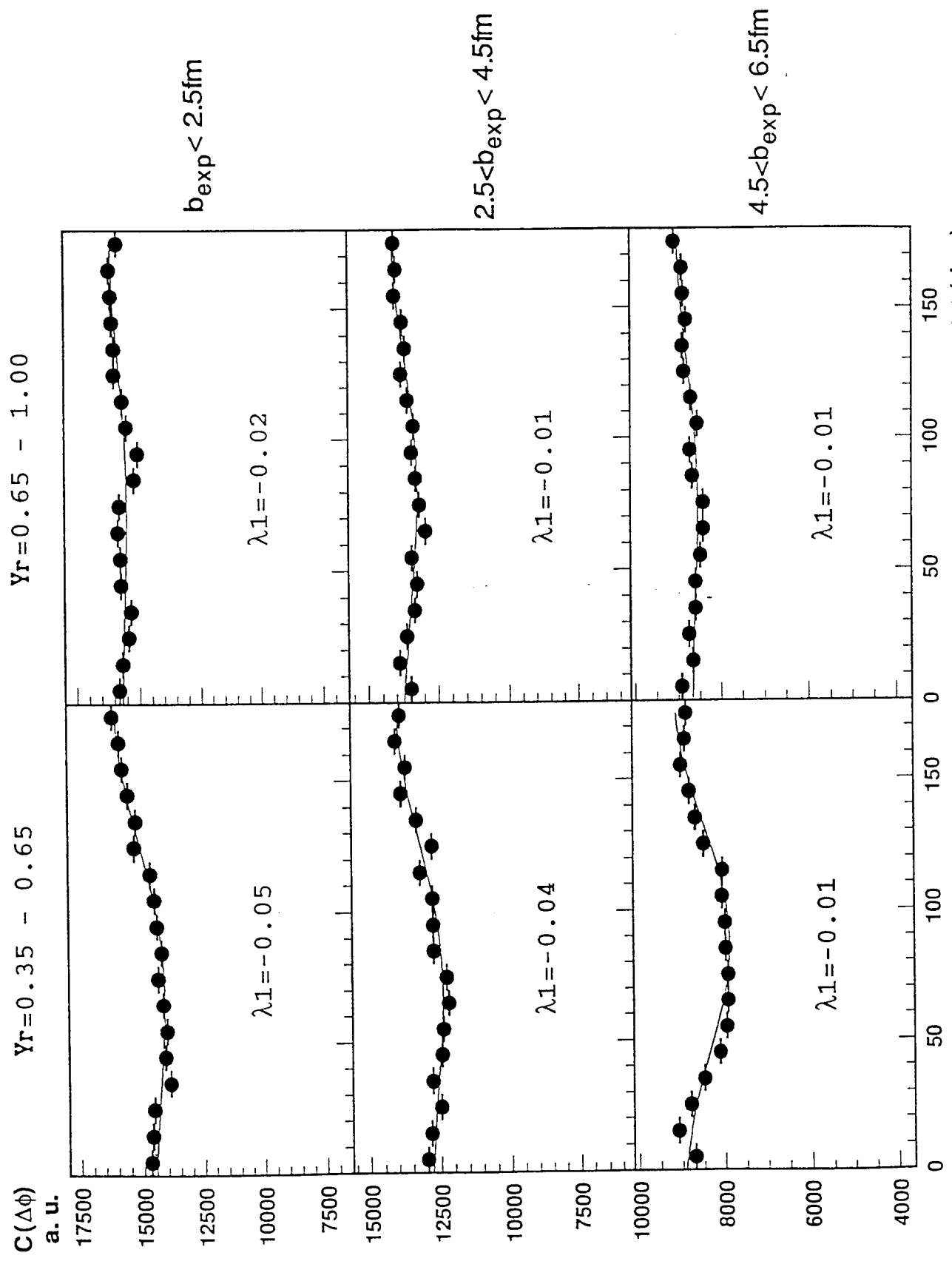


Figure 3

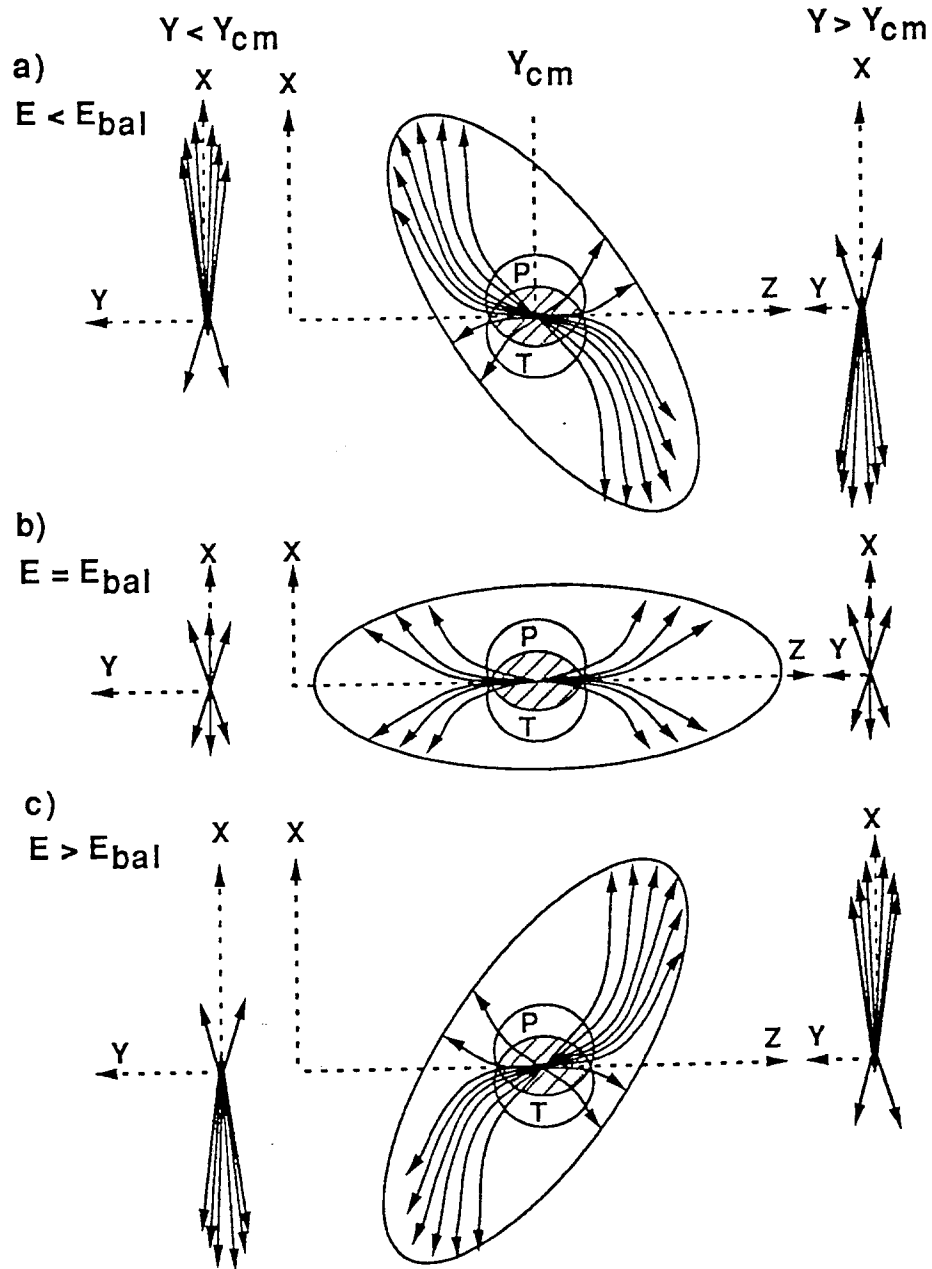


Figure 4

MULT=6

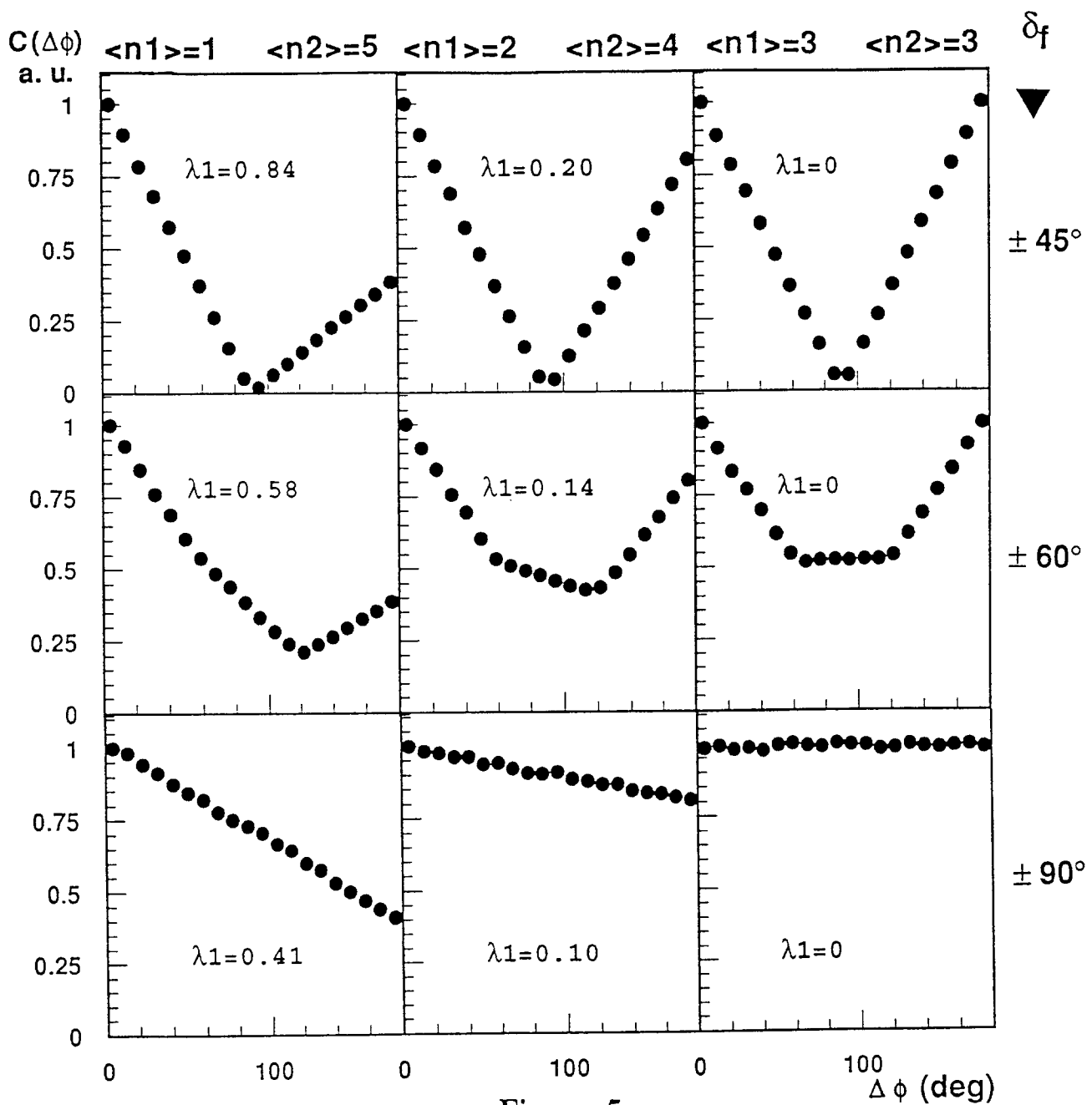


Figure 5

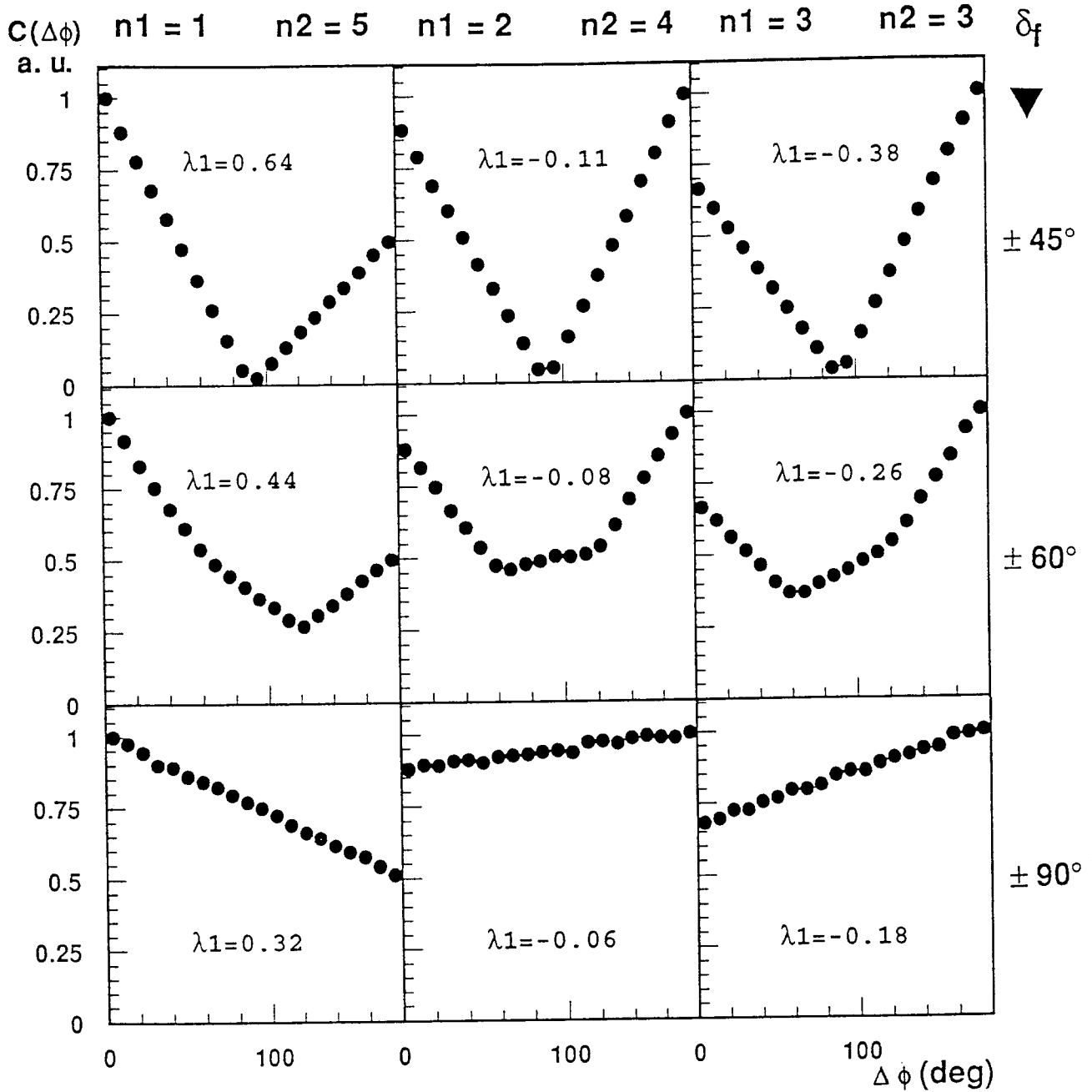
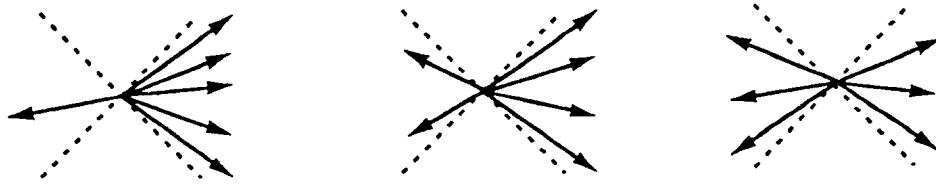


Figure 6

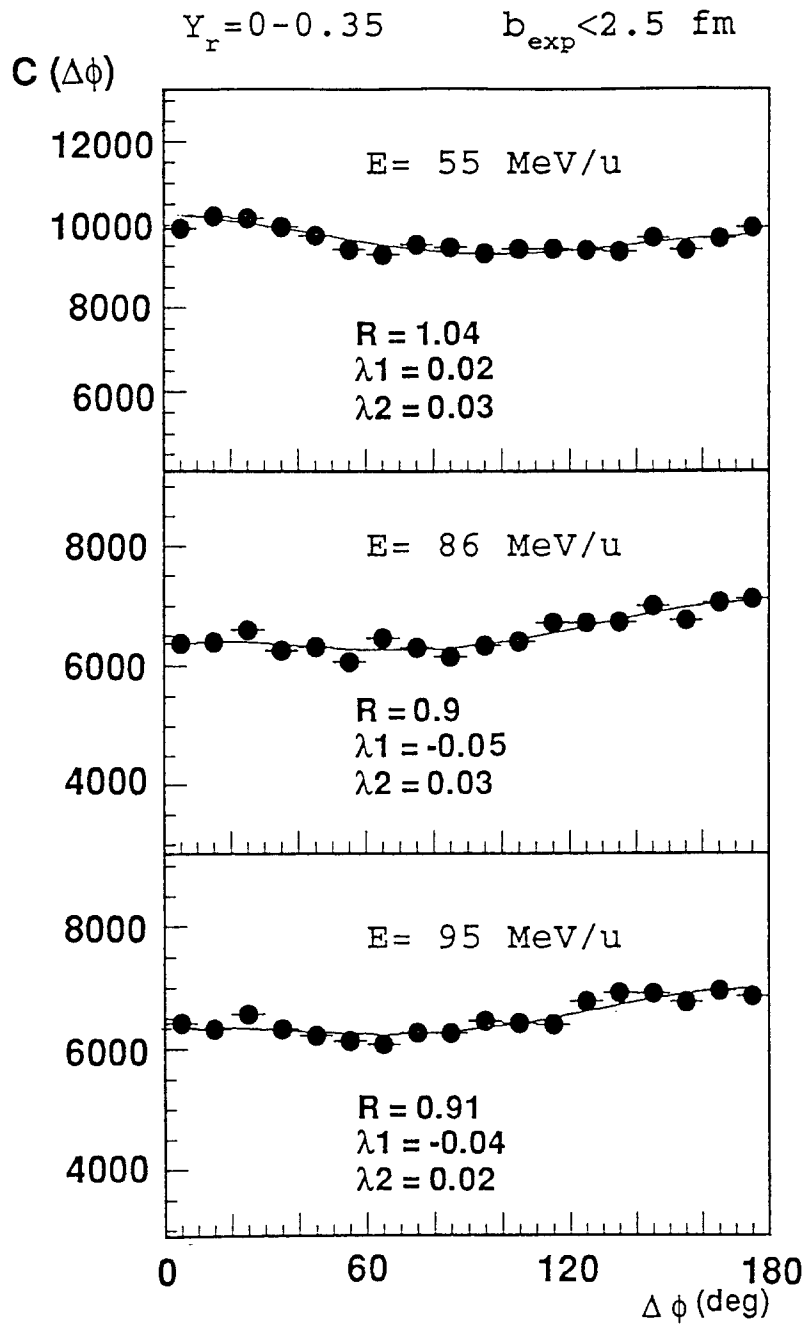


Figure 7

$$Y_T = 0.0 - 0.35$$

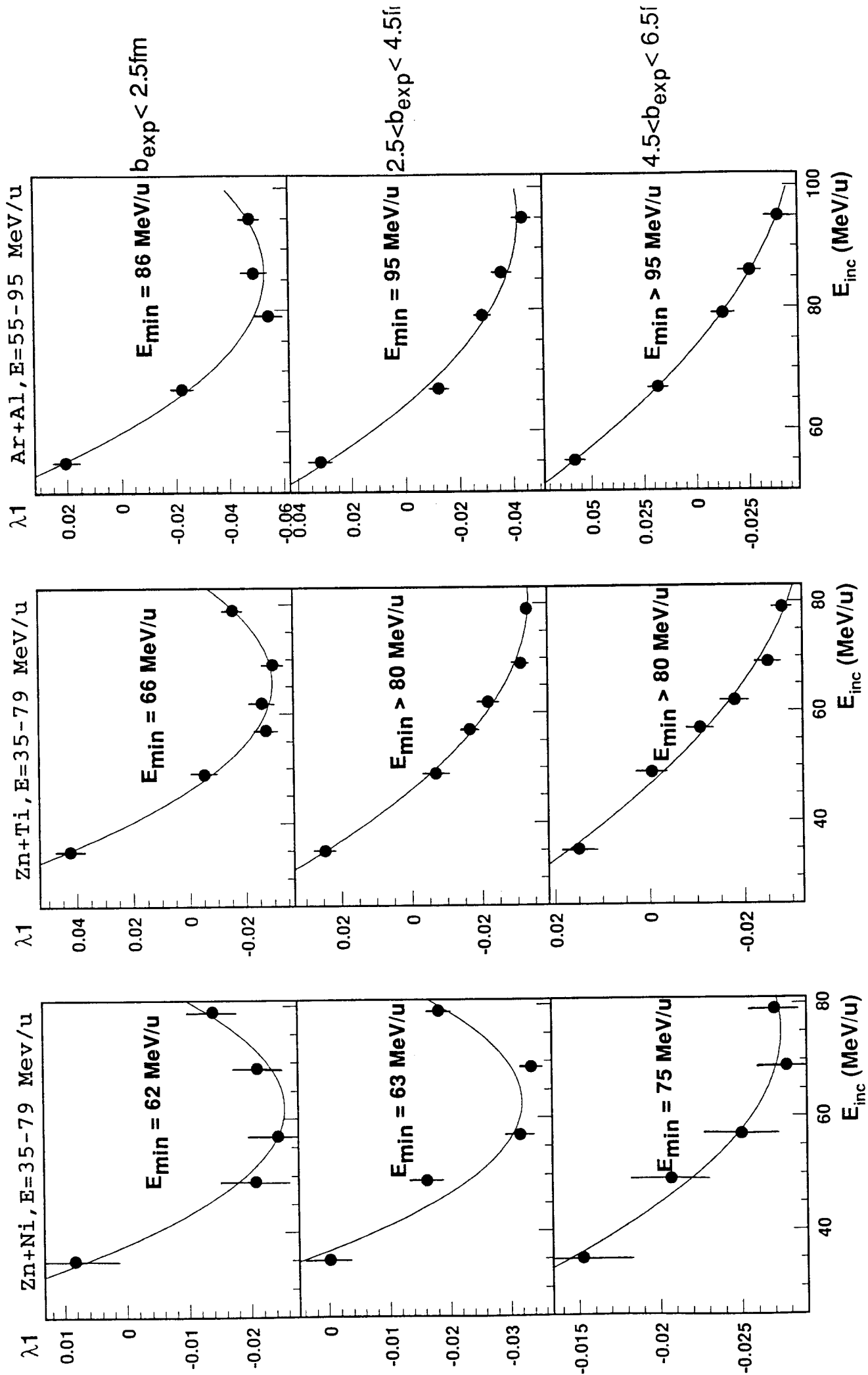
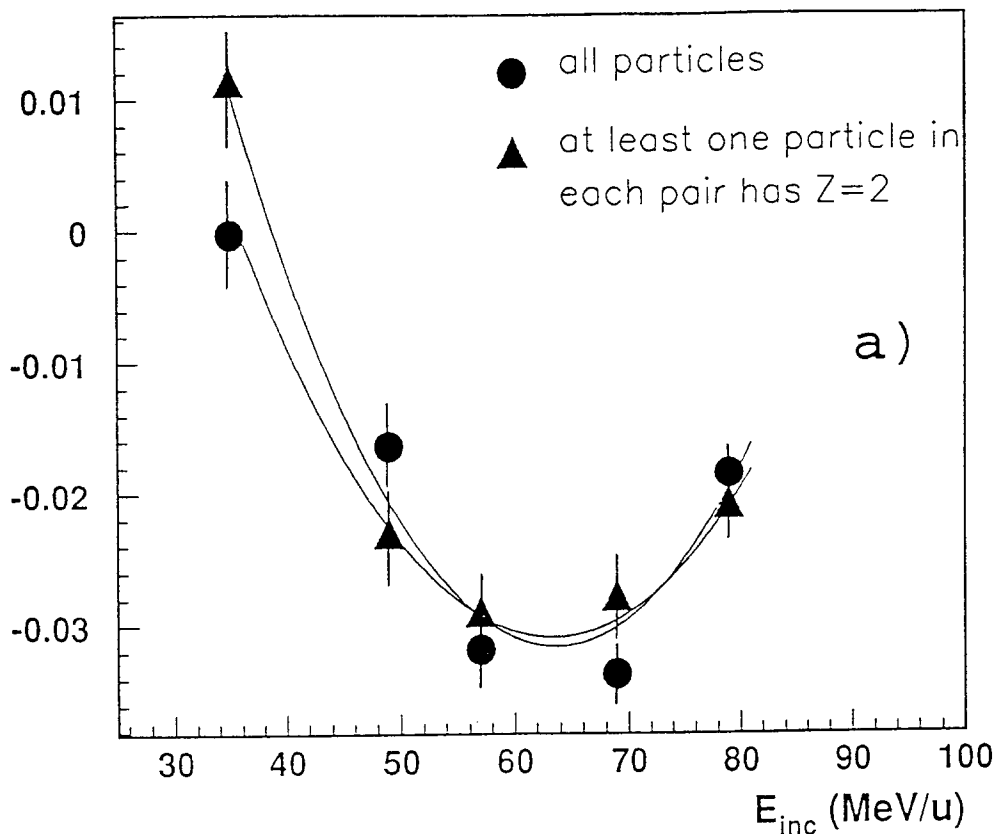


Figure 8



Zn+Ni  $2.5 < b_{\text{exp}} < 4.5$  fm



Ar+Al  $4.5 < b_{\text{exp}} < 6.5$  fm

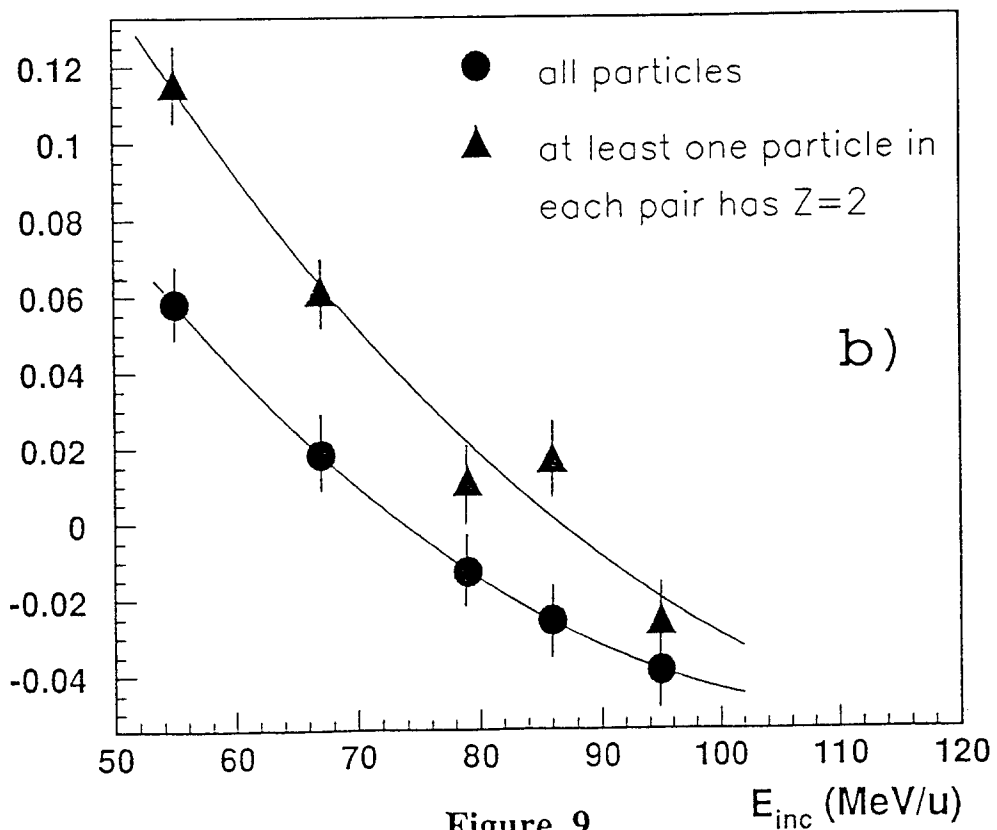


Figure 9

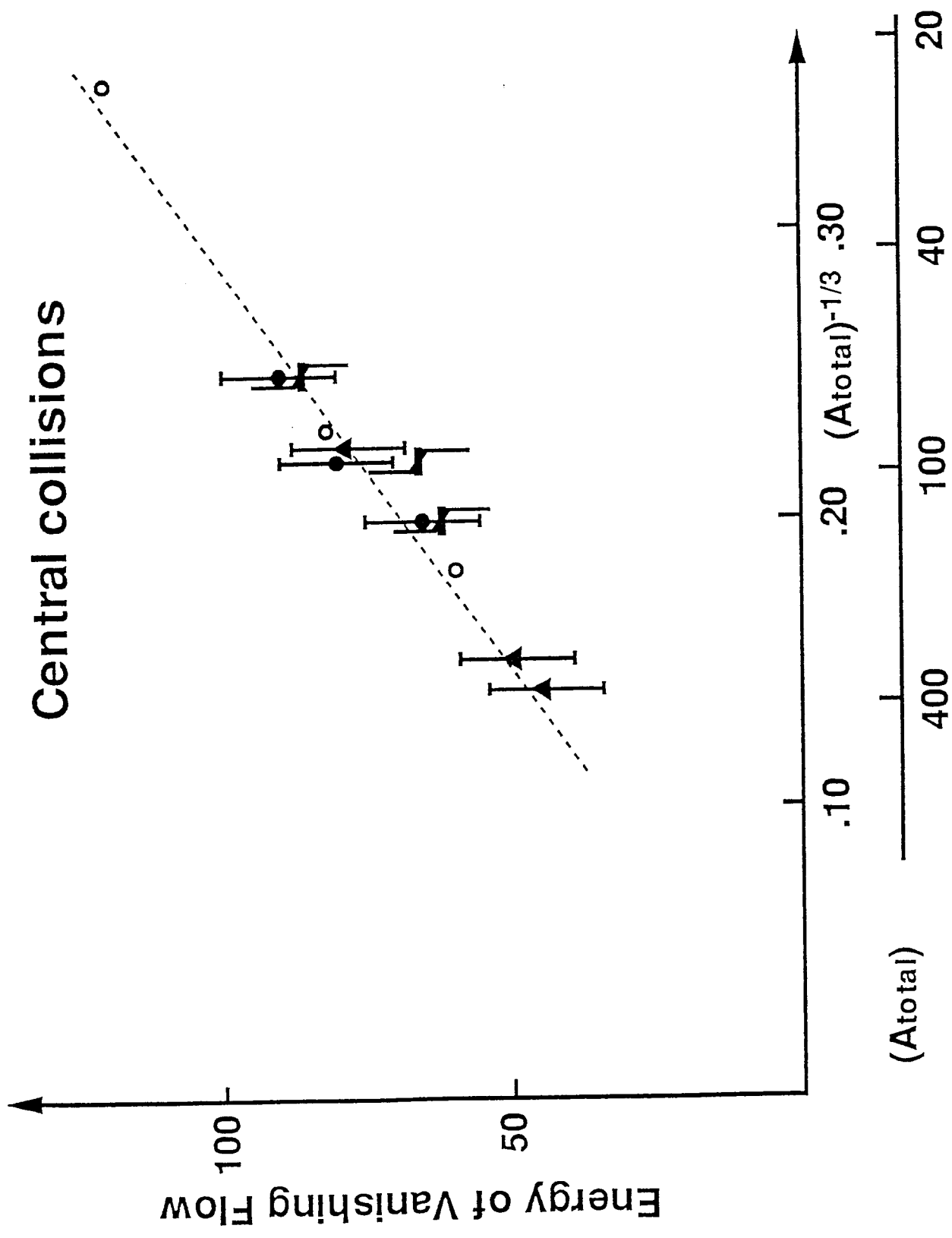


Figure 10

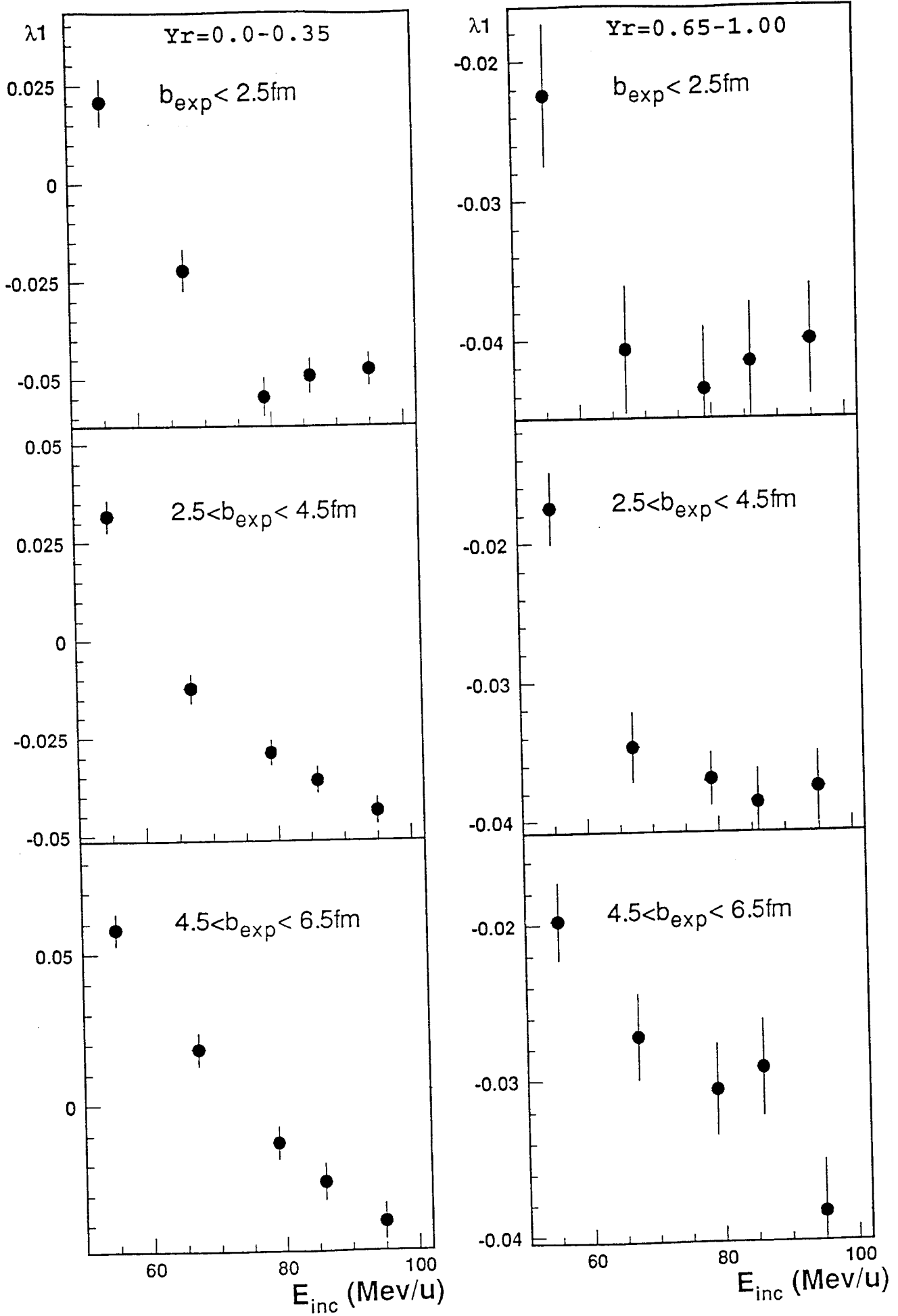


Figure 11

